NOAA Polar-Orbiting Operational Environmental Satellites (POES) Global Visible and Infrared Band Data from ESSA (1966 - 1972) and NOAA (1972 - 1978) Satellites

Campbell, G.G. 2019. NOAA Polar-Orbiting Operational Environmental Satellites (POES) Global Visible and Infrared Band Data from ESSA (1966 - 1972) and NOAA (1972 - 1978) Satellites. NOAA National Centers for Environmental Information. doi: https://doi.org/10.7289/V5QV3JV6.

Table of Contents

Data Description 2
- Summary 2
- Parameters 3
- File Information 5
  - Format 5
  - File Contents 5
  - Naming Convention 8
  - File Size 9
- Spatial Coverage, Resolution, and Projection 9
- Temporal Coverage and Resolution 10

Acquisition and Processing 12
- Background 12
- Acquisition 14
- Processing and Calibration 15
  - Analog Image Digitization Process 16
  - VIS Data Processing 17
  - VIS Data Normalization 18
  - IR Data Processing 18
  - IR Data Calibration 19
- Quality, Errors, and Limitations 20
- Instrumentation 20
  - ESSA Satellites 21
  - ITOS 1 and NOAA Satellites 21

Software and Tools 22
- Using Panoply 22
  - Plotting VIS Data 22
  - Plotting IR Data 23

Version History 23

Related Data Sets 23

Contacts and Acknowledgments 23

References 24
  - Additional References 25

Document Information 26
- Author 26
- Publication Date 26

Appendix - Quality Differences for 35 mm Film, Glossy, and Halftone 27

Data Description

Summary

This data set, NOAA Polar-Orbiting Operational Environmental Satellite (POES) Global Visible and Infrared Band Data from ESSA (1966 - 1972) and NOAA (1972 - 1978) Satellites, consists of daily visible-band (VIS) imagery from Environmental Sciences Service Administration (ESSA) satellites and the Improved TIROS Operational System 1 (ITOS 1) satellite, and both VIS and infrared-band (IR) imagery from National Oceanic and Atmospheric Administration (NOAA) satellites. Data from the ESSA series and ITOS 1 covers December 1966 through November 1972. Data from the follow-on NOAA series covers December 1972 through March 1978. The data set was created by scanning the analog imagery from these satellites held in the NOAA National Centers for Environmental Information (NCEI) physical archives in Asheville, NC. Images on 35 mm film, glossy prints, or paper halftone prints were scanned, processed, and then converted to NetCDF format.

NSIDC's goal was to convert these scanned images into a suitable format for those studying weather and climate between December 1966 and March 1978. These data are useful for validating reanalysis products, constructing cloud climatologies, and studying snow and sea ice distribution. See Figure 1 for an example comparing a reanalysis product with a visible-band example of reconstituted satellite imagery. Before this product's publication, the VIS data had not been available in any digital format. The IR data had been available as digital data on a coarse grid of 2.5° latitude by 2.5° longitude, or approximately 280 km in the north-south dimension (Liebmann and Smith, 1996). One objective of this project was to provide a digital VIS product and a digital IR product with better resolution and more months of data.

A note on data calibration: The National Institute of Standards and Technology (NIST) Handbook (HB) 157 describes radiometric calibration of remote-sensing instruments as a process of "evaluating the parameters required to understand and describe the performance of a sensor", leading to "the development of sensor-specific calibration equations that are used to convert the sensor output (in units of counts, volts, etc.) to the desired scientific data products" (Kacker and Yoon, 2015).

The analog images used for this data set are representations, of unknown fidelity, of the original sensor output. Calibration, strictly understood, cannot be performed on these data; but digitized image counts can be converted to equivalent long-wave radiation through a process of pseudo-calibration, in the case of IR, and to a normalized brightness, in the case of VIS, so that the data may be used for research purposes. In what follows, the term *calibrated* applies to data that have received this additional processing, and not to calibrated data as defined by NIST HB 157.

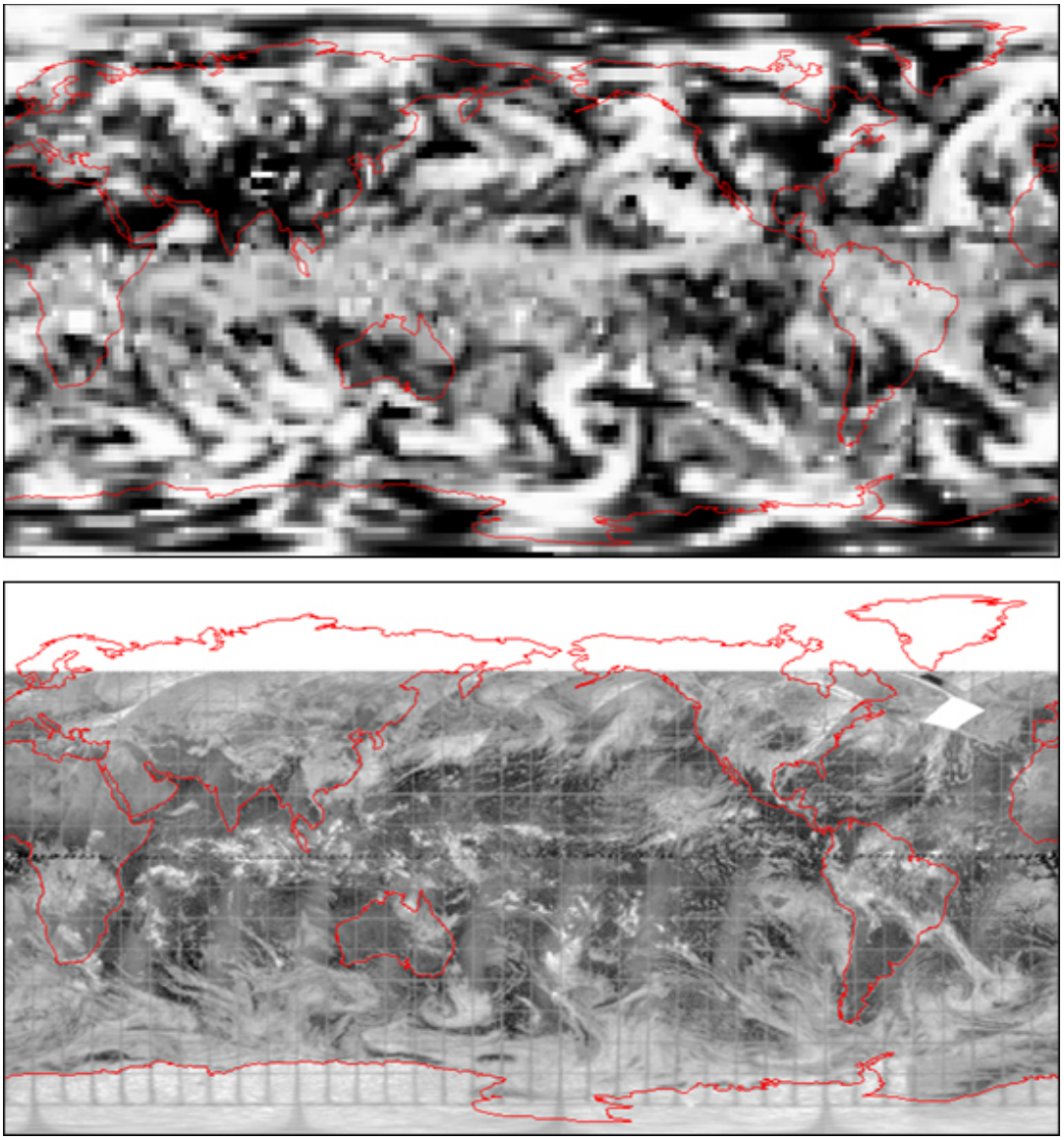

Figure 1. Cloud fraction from NCEP Reanalysis data (Kalnay et al., 1996) provided by NOAA/OAR/ESRL PSD, Boulder, Colorado, USA, from their website at https://www.esrl.noaa.gov/psd/ (top) and visible band NOAA 3 satellite imagery (bottom) from this data set. Both images show data from, nominally, 01 Jan 1975, but the satellite imagery is acquired over a 24-hour period that begins on 01 January and extends into 02 January.

Parameters

The two geophysical parameters provided with these data are visible-band (VIS) reflectance or brightness, given as a count in both normalized and raw forms; and longwave or infrared radiation (IR) in W/m^2, given as calibrated data as well as in a raw form. The parameters are described in Table 1 and are provided with a number of other variables in the NetCDF files, listed in Tables 2 and 3. Figure 2 is an example of an image of the VIS brightness, and Figure 3 is a daytime example of the IR data. Nighttime IR imagery is included but is not shown here.

Table 1. Parameter Description

Parameter	Description
Visible-band brightness	Normalized count of the brightness of the scanned VIS imagery. This parameter corresponds to the `vis_norm_remapped` variable in the VIS data files. The raw data equivalent is provided in the `vis_brightness_raw` variable. Data cover 01 December 1966 through 15 March 1978.
Longwave radiation (infrared band)	IR flux (W/m^2) that has been calibrated as described in the section on IR Data Calibration. This parameter corresponds to the `calibrated_longwave_flux` variable in the IR data files. The raw data equivalent is provided in the `IR_count_raw` variable. Data cover 06 December 1972 through 15 March 1978, with two files each day, one for daytime and one for nighttime.

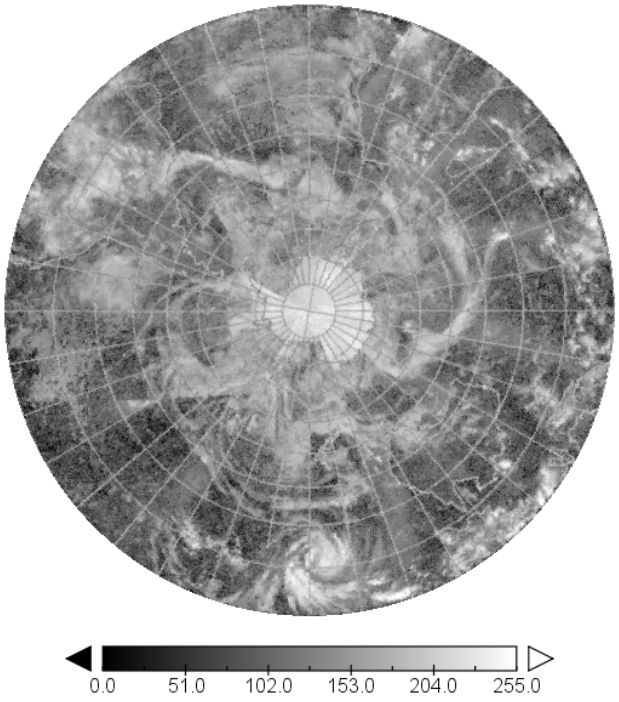

Figure 2. Example of VIS data file from the vis_norm_remapped variable for the Southern Hemisphere for 02 January 1978 (poes.NOAA-5.halftone.south.VIS.1978.01.02.nc). The image was made using the NASA Panoply tool.

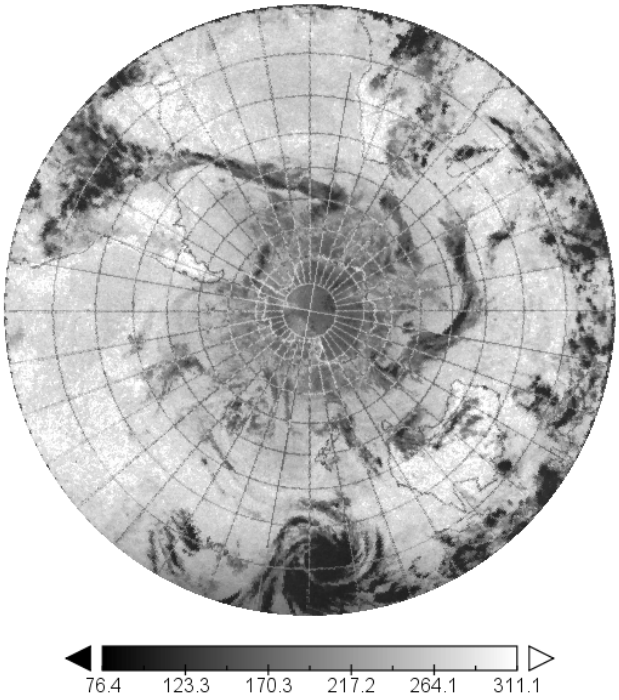

Figure 3. Example of daytime IR data from the calibrated_longwave_flux variable for the Southern Hemisphere for 02 January 1978 (poes.NOAA-5.halftone.south.IRday.1978.01.02.nc). The image was made using the NASA Panoply tool.

File Information

Format

The data files are in NetCDF4 format CF-1.7.

File Contents

For each hemisphere, there is a daily VIS file covering 01 December 1966 through 15 March 1978. From 06 December 1972 through 15 March 1978, in addition to VIS files, there are daily IR daytime and IR nighttime files. Files are grouped by satellite, sensor type, and month. There may be gaps in the daily series due to problems associated with poor quality or missing film.

Each NetCDF file contains both the calibrated data and the raw data from the original scans. The calibrated data have been georeferenced and mapped to a consistent grid. The raw data come directly from the scanned images which were digitized to varying resolutions. The variables in the VIS NetCDF files are described in Table 2 and the variables in the IR NetCDF files are described in Table 3. In Tables 2 and 3, fields annotated with a star contain data that are constant across all data files, for each hemisphere.

Table 2. Contents of VIS Data Files (in alphabetical order)

Variables	Description
count_normalization	Conversion table used to transform the raw data to the normalized brightness count. See the Acquisition and Processing section for details.
crs*	Coordinate reference system of the gridded data: Polar Stereographic.
crs_raw*	Coordinate reference system of the raw data: Polar Stereographic.
flag_raw	Quality flag for raw VIS data variable (`vis_brightness_raw`) 0 = good, 1 = off earth, 2 = poor quality
flag_remapped	Quality flag for calibrated VIS data variable (`vis_norm_remapped`) 0 = good, 1 = off earth, 2 = poor quality
lat*	Standard grid latitude
lon*	Standard grid longitude
orbit_limits	Beginning and ending orbit numbers taken from the hardcopy images. These were missing on approximately one third of the images. The value is set to zero in those cases.
raw_x*	The x projection coordinate for the raw data in meters.
raw_y*	The y projection coordinate for the raw data in meters.
time	Nominal date of the image in seconds since 1970-1-1 00:00:00. Note that the date can be negative with this NetCDF convention.
time_limits	Beginning and ending time of the satellite swaths in seconds since 1970-1-1 00:00:00.
vis_brightness_raw	Raw brightness greyscale count of the scanned VIS imagery.
vis_norm_remapped	Normalized count of the brightness of the scanned VIS imagery remapped to the standard grid. Valid data values range from 0 to 255. See the Acquisition and Processing section for information on how these were processed.
x*	The x projection coordinate for the remapped data in meters.
y*	The y projection coordinate for the remapped data in meters.

* Fields with a star contain data that are constant across all data files, for each hemisphere.

Table 3. Contents of IR Data Files (in alphabetical order)

Variables	Description
calibrated_longwave_flux	Calibrated IR flux (W/m^2). Valid scaled data values range from 0 to 400. Note, these data have been scaled (divided) by 50. Many NetCDF readers will automatically apply the scale factor and return the scaled data values. However, you may see values from 0 to 20000 depending on the NetCDF reader being used.
calibration_table	Conversion table for raw count to calibrated IR flux. See Acquisition and Processing for details.
crs*	Coordinate reference system of the gridded data: Polar Stereographic.
crs_raw*	Coordinate reference system of the raw data: Polar Stereographic.
flag_raw	Quality flag for raw IR data variable (`IR_count_remapped`) 0 = good, 1 = off earth, 2 = poor quality
flag_remapped	Quality flag for calibrated IR data variable (`calibrated_longwave_flux`) 0 = good, 1 = off earth, 2 = poor quality
IR_count_raw	Raw infrared greyscale count.
IR_count_remapped	Raw infrared count remapped to the standard grid.
lat*	Standard grid latitude
lon*	Standard grid longitude
OLR_longwave_flux	IR flux (W/m^2) from NOAA Outgoing Longwave Radiation (Liebmann and Smith, 1996) reference data set values. While these values have been mapped to the standard 10 km grid, they are from a data product at a much coarser resolution of 2.5˚ latitude by 2.5˚ longitude. Note, these data have been scaled (divided) by 50. Many NetCDF readers will automatically apply the scale factor and return the unscaled geophysical variable.
orbit_limits	Beginning and ending orbit numbers taken from hardcopy images. These were missing on approximately one third of the images. The value is set to zero in those cases.
raw_x*	The x projection coordinate for the raw data in meters.
raw_y*	The y projection coordinate for the raw data in meters.
time	Nominal date in seconds since 1970-1-1 00:00:00. Note that the date can be negative with this NetCDF convention.

time_limits	Beginning and ending time of the satellite swaths in seconds since 1970-1-1 00:00:00.
x*	The x projection coordinate for the remapped data in meters.
y*	The y projection coordinate for the remapped data in meters.

* Fields with a star contain data that are constant across all data files for each hemisphere.

Naming Convention

Files are named according to the following convention:
`poes.ssss-z.imagetype.hemisphere.BBBxxxx.YYYY.MM.DD.nc`

Table 4. File Naming Description

Variable	Description
poes	Indicates that data came from the Polar-Orbiting Operational Environmental Satellite program
ssss-z	Satellite series plus satellite number: ESSA (-3, -5, -7, -9), NOAA (-1, -2,-3,-4,-5), or ITOS (-1)
imagetype	The type of the original analog image: `halftone` or `film` (where `film` denotes both 35 mm film and glossy prints)
hemisphere	Indicates the hemisphere of the data in the data file: `north` or `south`
BBB	The band of the data: IR – infrared, VIS – visible
xxxx	Time of day of the data (this is for the IR data only): `day` or `night`
YYYY.MM.DD	Date of observation in the form 4-digit year, 2-digit month, and 2-digit day of month
.nc	Identifies this file as being a NetCDF file

File Size

The VIS data files are approximately 8 MB to 12 MB, and the IR data files are approximately 16 MB to 17 MB. The total volume of the data set is approximately 210 GB.

Spatial Coverage, Resolution, and Projection

This is a global data set with files for both the Northern Hemisphere and the Southern Hemisphere.

The analog hemispheric mosaics are in a polar stereographic projection (National Environmental Satellite Service, 1973). With this information, the scanned images were navigated to assign a geographic location to each pixel. The digital images were then remapped to the standard grid, with a projection chosen to match the original projection, and a grid cell size, or nominal resolution, of 10 km at the latitude of true scale. Table 5 provides grid details.

While the ground resolution of the visible band instruments was approximately 3 km and that of the infrared instruments was roughly 8 km (see Instrumentation section), the resolution achieved from scans of the analog film and prints was much coarser. The investigator chose a 10 km grid based on his qualitative judgement that features of about 10 km could be detected at mid-latitude in the image scans. A finer grid would have resulted in larger file sizes and grossly oversampled imagery, and a coarser grid would have resulted in under-sampling the scanned film and glossy prints. This does not apply to the halftone prints, which resolve features only as small as about 25 km across.

Note that the standard grid is 10 km in the north – south direction. However, grid cell dimensions increase from the nominal 10 km at the pole as latitude decreases as you go from the pole to the equator.

Table 5. Standard Grid Details

Nominal Grid Resolution	10,193.8 m
Grid Size (X x Y)	2600 x 2600
Projection	Polar stereographic
Latitude of True Scale	90.0° for NH, -90° for SH
Central Longitude (Meridian)	-80.0°
Central Latitude	North: 90.0° South: -90.0°
x-axis map coordinate of the center of the upper-left pixel	-13257043.5 m
y-axis map coordinate of the center of the upper-left pixel	13257043.5 m
Ellipsoid	Sphere

Units	meters

PROJ4 String	North:
	`+proj=stere +lat_0=90 +lon_0=-80.0 +lat_ts=90 +x_0=0 +y_0=0 +ellps=sphere +units=m +R=6371128`
	
	South:
	`+proj=stere +lat_0=-90 +lon_0=-80.0 +lat_ts=-90 +x_0=0 +y_0=0 +ellps=sphere +units=m +R=6371128`

Temporal Coverage and Resolution

The data span 01 December 1966 to 15 March 1978 at a daily resolution with occasional missing days (See Figure 4). VIS data are available from 01 December 1966 through 15 March 1978; IR data are available from 06 December 1972 through 15 March 1978.

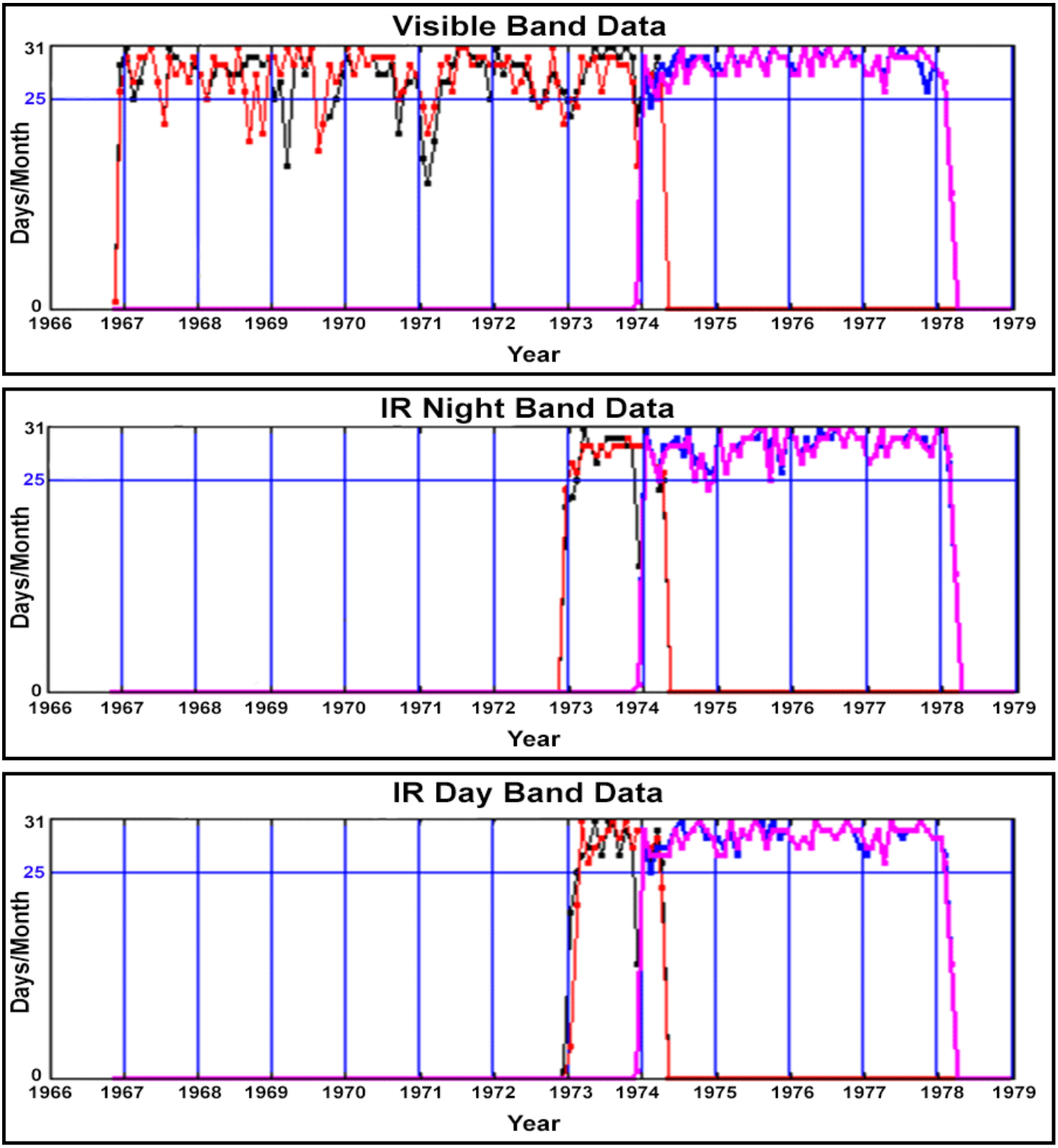

Figure 4. Days of data for each data type. Black/blue lines are the Northern Hemisphere, and red/purple lines are the Southern. Purple/blue lines are halftone prints and red/black lines are glossy prints/35 mm film. Notice the period in 1974 with all four.

Acquisition and Processing

Background

The ESSA agency was formed in 1965. ESSA satellites were the first operational meteorological satellites launched by an agency program committed to ongoing daily global observations. The series came after early research and development satellites, like the Television Infrared Observation Satellite (TIROS) series launched by NASA between 1960 and 1965. Massom (1991) outlines the applications that motivated U.S. agencies to develop these first polar-orbiting satellite capabilities in a chapter titled *History and development of satellite-borne polar remote sensing*, and provides details on how TIROS, ESSA, and ITOS satellites evolved. ESSA was a precursor organization to NOAA; and following NOAA's establishment in 1970, the NOAA satellite series was launched. NOAA 2 was the first meteorological satellite to use a scanning radiometer rather than a camera, and with NOAA 2, "the semi-quantitative use of satellite data to study the large-scale behavior of snow and ice masses for both operational and research purposes" became a reality (Massom, 1991).

The ESSA satellites, the ITOS 1 satellite (also known as TIROS M), and the NOAA 1 satellite were in operation from 1966 through 1971. ESSA 1, 3, 5, 7, and 9 were equipped with the Advanced Vidicon Camera Subsystem (AVCS). The AVCS, developed by NASA, was also used on the Nimbus 1, 2, and 3 satellites, which began recording data in 1964 (see Related Data Sets). The AVCS acquired visible-band data; the quality of the resulting imagery varied throughout the period of operation.

AVCS-equipped odd-numbered ESSA satellites recorded data for playback to ground-stations at Wallops Island, Virginia, and Gilmore Creek, Alaska. In the mid-1960s, ESSA implemented a computer program to composite AVCS image frames into hemispheric polar-stereographic mosaics of the Earth. See National Environmental Satellite Service (1970) and the references therein. This computer program collected the digital data, which covered small square portions of the Earth (Figure 5 left), and merged them into full hemisphere-wide composites, one for the Northern and one for the Southern Hemisphere (Figure 5 right). Between 12 and 13 orbits of observations and on the order of 100 square frames were combined into these two hemispheric images.

Note: Even-numbered ESSA satellites (ESSA 2, 4, 6, and 8) also existed but transmitted imagery directly to receiving stations by Automated Picture Transmission (APT). AVCS imagery from the odd-numbered ESSA satellites came with embedded coastlines and graticules (Figure 5 left) and were assembled into mosaics by NOAA, whereas APT imagery is not available as mosaics and comes without means to easily geolocate individual image frames. This data set uses only AVCS imagery.

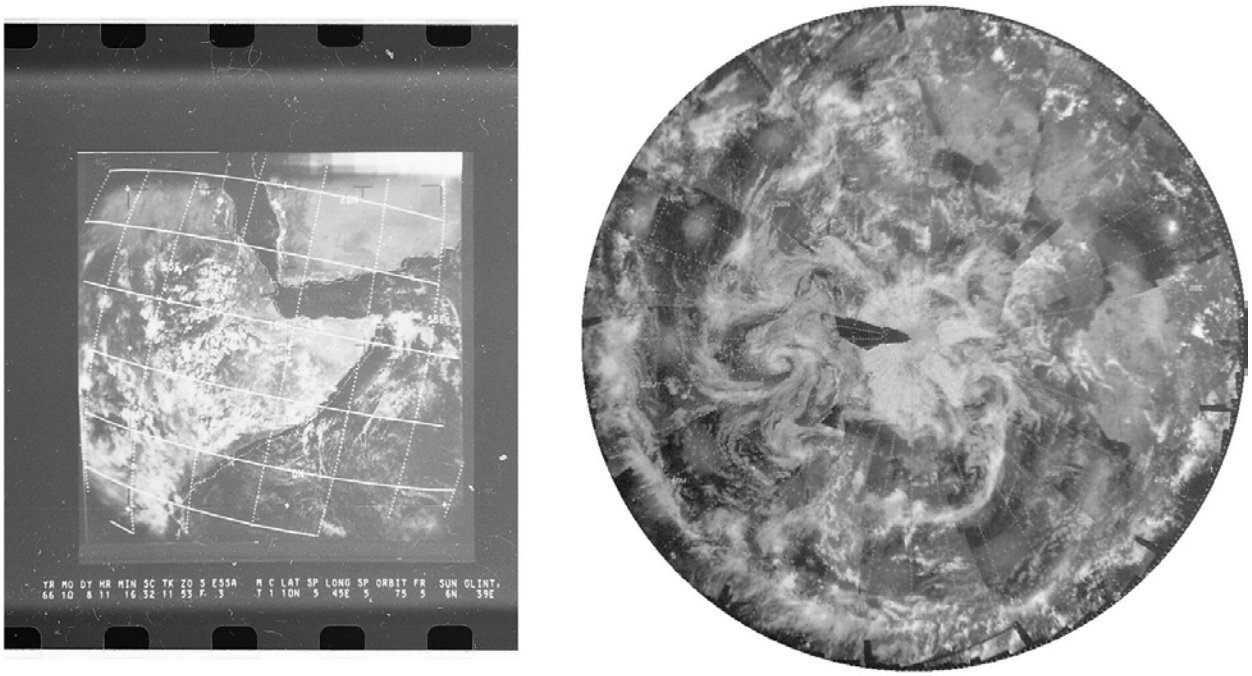

Figure 5. Individual 35 mm film frame (left) from the AVCS onboard an ESSA satellite. Multiple frames composited together form a hemisphere-wide image (right). Cloud distributions, land surfaces, and sea ice are visible.

In 1972, NOAA launched a new series of satellites (NOAA 2, 3, 4, and 5) that included a scanning radiometer (SR). This provided VIS data that were converted into pictures much like the ESSA products. In addition, the SR acquired infrared data that were mapped into day and night global polar-stereographic images with gray scales proportional to temperature (Massom, 1991). NOAA 5 operated through July 1979, however, only data through March 1978 are included in this data set.

Note that ITOS 1 and NOAA 1 had an SR as well as an AVCS instrument. However, only VIS imagery from ITOS 1 and NOAA 1 are included in this data product, and whether the instrument producing it was the SR or the AVCS is unknown. See the Instrumentation section for individual satellite operational dates and orbital characteristics.

The *Key to Meteorological Records Documentation Series* provides additional information on satellite instrumentation and on how the SR data were processed and mosaics constructed. From number 5.4 in that series (National Environmental Satellite Service, 1973):

> Visible and infrared data swaths obtained while the satellite is southbound on the daylight side of the orbit are used in the 09L mosaics; infrared data swaths obtained during northbound passage are used in the 21L mosaics. The scan-line signals are digitized, earth located, and repositioned on a standard polar stereographic map projection. Coastal outlines and latitude/longitude lines are added by the computer. Overlap between successive swaths is eliminated, with the latest data retained.

The daily mosaics are derived from data swaths beginning near 20 E longitude and progressing westward through the 24 hour period to the latest swath of the day near 30 E.

The imagery from these satellites was archived on 35 mm film and 11 in x 11 in glossy prints, and published in U.S. Department of Commerce monthly reports as halftone prints. This archive of analog images is housed at NOAA NCEI in Asheville, NC.

The ESSA, ITOS, and NOAA satellites were part of a POES system of satellites with a meteorological mission that continues to this day as a cooperative program between NOAA, NASA, and international partners. The images in this data product provide observations of the daily weather in the decade before the POES series was instrumented with the broad-band Advanced Very High Resolution Radiometer (AVHRR). The AVHRR record began in November 1978 and continues at least through the publication date of this document. NASA Goddard Space Flight Center maintains a timeline of most POES satellite launches from the beginning in 1960 through the 2018 launch of the third European Space Agency Met-Op satellite (site accessed 14 May 2019).

The Nimbus series of NASA research and development satellites, in orbit in the 1960s and 1970s, also acquired VIS and IR imagery. Imagery from Nimbus 1, 2, and 3 has been recovered through a project similar to that which produced this data set. Data from August 1964 to March 1971 are available from the NSIDC DAAC on the Nimbus Data Sets web page.

Acquisition

Black and white 35 mm film, 11 in X 11 in glossy prints, and paper halftone prints (Figure 6) were scanned at both NCEI and NSIDC. At NSIDC, undergraduate students did much of this work. The highest quality results came from the glossy prints. The halftone prints came from U.S. Department of Commerce monthly reports like those in National Environmental Satellite Service (1973). See the Appendix for a comparison of the quality of the 35 mm film, glossy prints, and halftone prints.

Unfortunately, the glossy prints and 35 mm film covering 1975 through 1978 were not preserved in the NCEI archive; only the halftone prints were retained. Prior to 1975, glossy prints were available. If there were missing days in the glossy prints, the 35 mm film scans were used to fill in the time series. For January, February, March, and April of 1974, both glossy and halftone prints were available from the analog archive, so both were scanned and provided in this data set. Most users will want to use only the data from glossy prints, however, we include those from halftone as well so that the two can be compared in this overlap period.

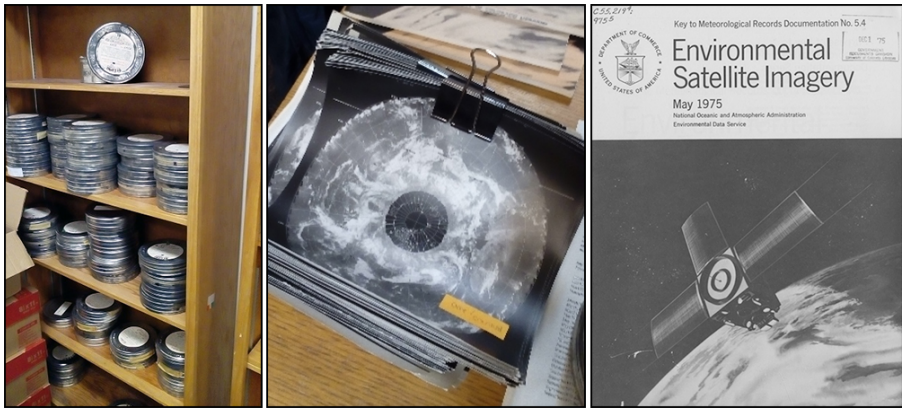

Figure 6. These three pictures show the film canisters (left), the glossy prints (middle), and the monthly reports containing the halftone prints (right).

Approximately 90% of the daily images have been recovered. Missing days are scattered through the time series at random (Figure 4). We note that if the glossy prints from the 1975 to 1978 SR instrument could be found and digitized, those prints would improve the quality and temporal resolution of the products for that time period.

This data set begins with ESSA 3 in December 1966. ESSA 1 had an AVCS that acquired images earlier in 1966. These pictures are archived at NCEI in Asheville, NC as individual frames and not as hemisphere-wide mosaics like the other analog images used in this data set. NSIDC personnel looked at some of these images but were not able to reconstruct the navigation for the individual frames to create hemispheric composites. Some future researcher might be able to use these individual frames for climate studies. Data from Nimbus 2 cover some of the time period covered by ESSA 1. See the Nimbus Data Sets web page for more information.

Processing and Calibration

Processing and calibration consisted of these steps:

- Digitize (scan) analog images. Note: This was done at sufficient pixels per inch to resolve features as small as about 10 km across. See the section on Spatial Coverage, Resolution, and Projection for more information.
- Add geolocation information to the scanned hemispheric mosaic. Adding geolocation information is sometimes called navigating the image.
- Map the image data to a standard polar stereographic grid. Table 5 has grid and projection parameters.
- Normalize or calibrate the imagery using a variant of the image processing technique of histogram matching:
    - For VIS data, this was done by normalizing the brightness counts to a monthly standard cumulative frequency distribution.
    - For IR data, this was done by directly comparing brightness counts in each image with a reference data set.
- Save each digital image to a NetCDF file. Each file contains both processed and raw versions of the data.

These steps are described in more detail in the sections below.

Analog Image Digitization Process

1. *Scan*: Image scanning, of both the VIS and IR images, took place at NCEI in Asheville, NC and at NSIDC in Boulder, CO. The black and white glossy prints and halftone prints were scanned with an Epson scanner. The 35 mm film was scanned with a Wolverine F2D Mighty film to digital converter. The scans were originally saved as color images in one of three formats: .png, .jpg, or .pdf. The full resolution size of these images, in pixels, varied. Ideally, images would have been scanned and saved as grey-scale images in .tif format, but limitations of the scanners made this difficult.

2. *Convert color to greyscale*: Green channel counts were used for greyscale counts. These were extracted from the RGB image files using routines from the Java image IO library. These fall within a range of 0 to 255.

3. *Navigate the scanned hemispheric mosaics*: To orient the raw grid arrays where each image pixel is the equivalent of a grid cell, each image was displayed on a computer monitor, and a human inspected the images to pick out three points on the equator grid circle (Figure 7, red stars). The three points established the center of the circle defined by the equator; and thus, the location of the pole on the image grid. Next, a point on a line of longitude was chosen (10° E was used in the Northern Hemisphere, Figure 7, blue star), and its X-Y position was determined. This, along with the X-Y position of the pole, was used to find the relative angle of rotation of each image through simple trigonometry. This was enough information to determine the polar stereographic projection and grid parameters and finally the latitude and longitude of every point in the image.

4. *Flag bad data*: Images were reviewed and areas of off-Earth and missing or poor-quality data were marked (Figure 7, green areas). These were flagged in a flag variable with a value of 1 for off-Earth or 2 for missing or poor-quality data. Poor-quality data may arise from several causes. Among them are missing orbits, corrupted data transmissions from the satellites, and inaccurate navigation information. Note that bright and dark segments appear in some images and seem to be artifacts of how the original film record was processed or printed. Data are flagged rather than removed, so that users may choose to include or omit them from analyses. Some missing or poor-quality data may have escaped this processing step. Note that the graticule and coastlines are embedded in the images as dark lines and light lines, respectively, and the greyscale counts that mark them are not flagged and cannot easily be removed.

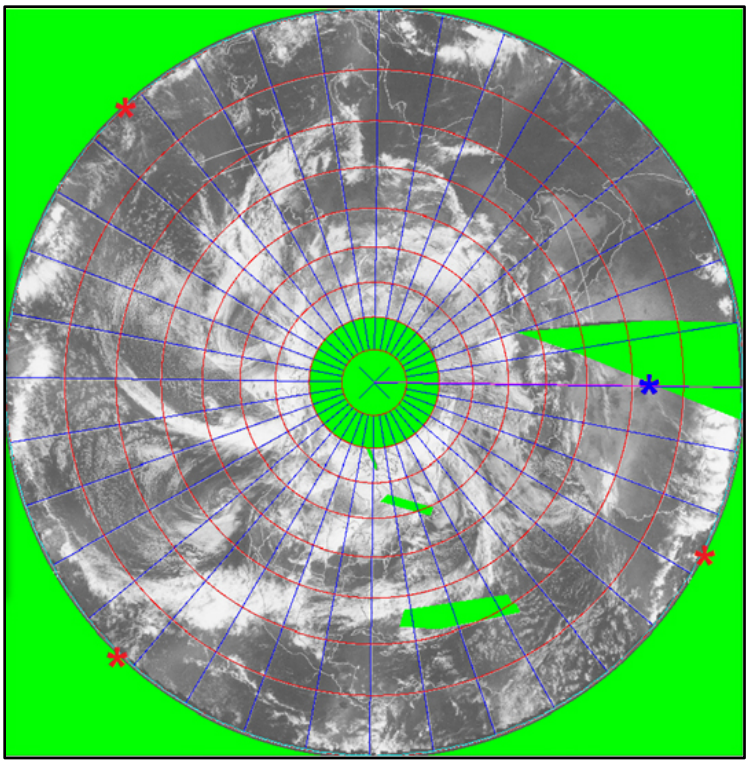

Figure 7. Poor-quality or off-Earth data pixels were flagged (green), three points on the equator grid circle were selected (red stars), and a point that indicated the horizontal (10° E) was selected (blue star).

VIS Data Processing

Once digitized, the VIS files were processed further as follows:

1. *Construct cumulative frequency distribution*: A cumulative frequency distribution was derived from the area of good quality data from 0° to 30° N, or 0° to 30° S, for each image.

2. *Construct normalization table*: Each image's cumulative frequency distribution was matched to that month's standard distribution. The standard distribution was used to arrive at a conversion table for raw counts to normalized counts for the image. The NetCDF `count_normalization` variable, in the VIS files, holds this table. See the VIS Data Normalization section for more information.

3. *Regrid and normalize*: To arrive at the final product, each image file was remapped to the standard projection and grid using the nearest neighbor method to fill grid cells, and the normalization table applied to all grid cell count values in the image. This yields 8-bit byte arrays that, when displayed as images, are roughly consistent in overall brightness over the entire data set.

4. *Smooth halftone-print-derived images*: Images from halftone prints have been smoothed with a 7-point smoothing filter. This was done to remove the black dots that characterize halftone printing, and, in some cases, artifacts such as a moiré pattern that can appear when halftone prints are reprinted.

VIS Data Normalization

No firm reference radiance or albedo data are available with which to calibrate the VIS data, and photo processing and printing were not consistent over the time series. To address these factors, the empirical approach of histogram matching was used. Each value in the image to be normalized was matched to the value having the same probability in the standard distribution for that month and hemisphere. The procedure yielded a look-up table, unique to each image, for converting raw counts to normalized counts. The standard cumulative frequency distributions, 24 in all, were derived using data from 0° to 30° North or South latitude only, in order to omit polar regions which are dark during the polar night and saturated bright during the polar day.

Figure 8 illustrates the method. Normalizing image brightness in this way did not strictly calibrate the images, but it greatly reduced variability in the range of image brightness from day to day over the entire data set.

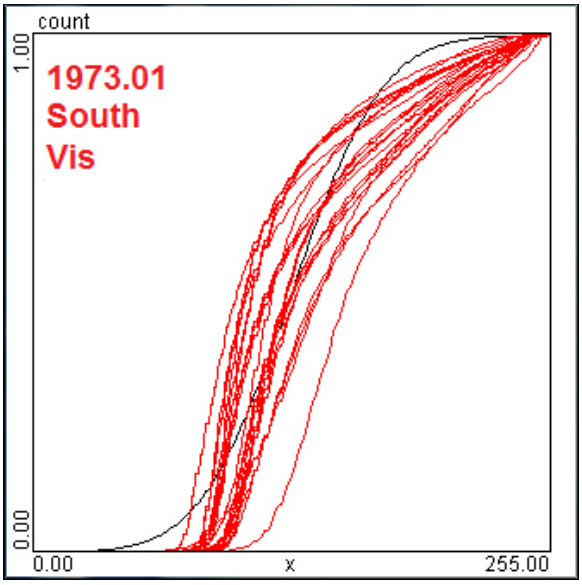

Figure 8. In this example from the Southern Hemisphere in January of 1973, the cumulative frequency distributions from the raw data between the equator and 30° S for each day are shown in red. The January Southern Hemisphere standard cumulative frequency distribution is shown in black.

IR Data Processing

Once digitized, the IR files were processed further as follows:

1. *Regrid and scale*: The imagery was remapped to the standard projection and grid using the nearest neighbor method to fill grid cells and stored as an array of floating-point numbers in the NetCDF product files. These numbers have been scaled (divided) by 50. The reference Outgoing Longwave Radiation (OLR) data were remapped as well and also stored in the NetCDF files.

2. *Construct cumulative frequency distribution*: As with VIS image processing, a cumulative frequency distribution was derived from the area of good quality data from 0° to 30° or 0° to -30° latitude for each image.

3. *Construct calibration table*: Each image's cumulative frequency distribution was matched to a cumulative frequency distribution for the same day derived from the NOAA OLR data set (Liebmann and Smith 1996). This served as a conversion table between counts and OLR W/m^2 floating point numbers. The NetCDF `OLR_longwave_flux` variable, in the IR files, holds this table. See the IR Data Calibration section for more information.

4. *Smooth halftone-print-derived images*: A 7-point smoothing filter was applied. This was done to remove the black dots that characterize halftone printing, and, in some cases, artifacts such as a moiré pattern that can appear when halftone prints are reprinted.

IR Data Calibration

Calibration of the IR data was achieved by comparing the scanned IR images to the reference OLR data set (Liebmann and Smith 1996). These calibration data, remapped from their 2.5° latitude by 2.5° longitude grid to this product's standard grid, and divided by a scale factor of 50, are available in the `OLR_longwave_flux` variable in the IR files.

Note: The OLR data came from the same raw satellite data feed as the gray-scale IR images. In the 1970's, the SR IR-band swath data were remapped from their native resolution of about 8 km at nadir to a 2.5° latitude by 2.5° longitude gridded product: the OLR data. The OLR data grid cells are about 280 km in the north – south dimension. The OLR data product has been widely used in the years since its creation.

The best match between the OLR and the scanned images was obtained with a one day offset between the labeled image times. This serves as a reminder that mosaic images are not snapshots, but are composites of between 12 and 13 orbits of data, acquired over approximately 24 hours. One must take care to be aware of the time of observation when comparing with other daily data.

OLR data are available for direct calibration of IR images from June 1974 and later. For the period December 1972 through May 1974, there are no available OLR data. To calibrate IR images during this time period, an average OLR image was prepared using OLR data from the same calendar day over June 1974 into March 1978. This provided a seasonally varying standard OLR field for comparison with IR data.

Note that a legend appears on some of the IR images as a grey wedge, with coarse temperature values corresponding to different gray scale values. This gray wedge did not prove useful for calibration.

Quality, Errors, and Limitations

The satellites were in sun synchronous orbits with an afternoon equator crossing time. Low solar elevation reduces image quality, especially near the poles, where a strong cross-track gradient is evident in each orbit's swath. View angle and illumination angle effects are apparent in the visible-band imagery. This is more noticeable in the Southern Hemisphere observations. Massom (1991) notes that many important polar features are not resolved, and areas of low ice concentration or new ice are difficult to detect in ESSA and NOAA satellite imagery. One can see seams between orbits because clouds and other weather patterns change in the 100 minutes between orbits. Note, too, that if one remaps the data into an equatorial projection, there is a seam of missing data at the equator.

The IR data are hampered by poor resolution, and in summer, melt conditions may make image interpretation difficult.

Images have imbedded graticules of latitude and longitude and continental boundaries. The students who navigated the images used these when choosing tie points with which to geolocate the digitized pixels. However, they do contaminate the greyscale data, and the imbedded dark lines should be considered before carrying out any automatic analysis.

NSIDC has reviewed all the images and flagged regions with obvious problems associated with poor-quality data. These occur because of missing orbits, noise in data reception from the satellite, or remapping error.

Instrumentation

The ESSA and NOAA satellites were operational from 1966 through 1978. Table 6 lists the specific operational dates of each satellite in the ESSA and NOAA series that were used in this data set. Massom (1991) includes more information about these satellite series and their instrumentation, with a focus on their utility in polar regions, along with background information on the programs that supported them and their contribution to polar remote sensing.

Table 6. Satellites and Instruments Used, with Operational Dates
Note: The operational dates are the dates that the satellite was recording data and not necessarily the dates of the data that are used in this data set.

Satellite	Operational Dates	Instrument
ESSA 3	02 October 1966 - 02 December 1968	AVCS
ESSA 5	20 April 1967 - 20 February 1970	AVCS
ESSA 7	16 August 1968 - 10 March 1970	AVCS
ESSA 9	26 February 1969 - 12 November 1972	AVCS
ITOS 1	23 January 1970 - 18 June 1971	AVCS or SR (uncertain)

NOAA 1	11 December 1970 - 19 August 1971	AVCS or SR (uncertain)
NOAA 2	15 October 1972 - 30 January 1975	SR
NOAA 3	06 November 1973 - 31 August 1976	SR
NOAA 4	15 November 1974 - 18 November 1978	SR
NOAA 5	29 July 1976 - 16 July 1979	SR

ESSA Satellites

This data set contains data from the ESSA 3, 5, 7, and 9 satellites. These data were collected with the AVCS instrument onboard the ESSA satellites. It captured pictures in the visible wavelength band from 0.45 µm - 0.65 µm with a ground resolution of 2.2 km - 3.0 km and a swath width of 2300 km (Massom, 1991). Table 7 provides orbital characteristics of the ESSA satellites.

Table 7. ESSA 3, 5, 7, and 9 Satellite Orbital Characteristics

Orbital Characteristic	Description
Semi-major axis	7,152 km - 7,846 km
Orbital height	702 km - 1,508 km
Inclination	97.9° - 102.12°
Period	100.35 - 115.28 minutes

ITOS 1 and NOAA Satellites

This data set contains data from ITOS 1 and NOAA 1, 2, 3, 4, and 5 satellites. These satellites were equipped with the SR instrument and ITOS 1 and NOAA 1 also carried the AVCS instrument. The SR captured images in the visible and infrared wavelength bands, 0.50 µm - 0.70 µm and 10.50 µm - 12.50 µm, respectively, with a 2900 km swath width and a ground resolution of 3.2 km for VIS and 8.0 km for IR (Massom, 1991). Equator crossing time was 0900 local time for daytime VIS and IR, and 2100 local time for nighttime IR (National Environmental Satellite Service, 1973). Table 8 provides orbital characteristics for the ITOS and NOAA satellites.

Table 8. ITOS 1 and NOAA 1, 2, 3, 4, and 5 Satellite Orbital Characteristics

Orbital Characteristic	Description
Semi-major axis	7,575 km - 7,894 km
Orbital height	918 km - 1,522 km
Inclination	97.9° - 102.80°
Period	109.36 - 116.34 minutes

Software and Tools

There are a number of NetCDF file readers available to read/view NetCDF files. For a list of some of these tools, please see the NetCDF Resources at NSIDC: Software and Tools Web page.

Using Panoply

Panoply is a JAVA application developed by NASA for viewing NetCDF files. This section describes how to use Panoply to read and visualize the NetCDF data files in this data set. For more information and to download a copy of Panoply, visit NASA's Panoply NetCDF Viewer Web page.

Plotting VIS Data

1. Open a VIS data file - file names like `poes.NOAA-5.halftone.south.VIS.1978.01.02.nc`
    a. Launch Panoply.
    b. From the **File** tab, select **Open** and then navigate to the VIS file you wish to open.
    c. Select the file and click **Open**.
2. Plot the `vis_norm_remapped` variable.
    a. In the Panoply window with the list of NetCDF data fields, double click on **vis_norm_remapped**.
    b. The **Create Plot** dialog box will appear. The **Create a georeferenced Longitude-Latitude plot** radio button should already be checked by default.
    c. Click **Create**.
3. Format the plot area.
    a. In the plot window, select the **Map** tab.
        i. From the **Projection** drop down, select **Stereographic**.
        ii. If you are plotting Northern Hemisphere data, set **Center on: Lon.** to -90 and **Center Lat.** to 90. If you are plotting Southern Hemisphere data, set **Center on: Lon.** to 0 and **Center Lat.** to -90.
    b. Select the **Scale** tab in the plot window.
    c. In the **Color Table** drop down, select **grayscale.act**.

Plotting IR Data

1. Open an IR data file - file names like `poes.NOAA-5.halftone.south.IRday.1978.01.02.nc`
    a. Launch Panoply.
    b. From the **File** tab, select **Open** and then navigate to the IR file you wish to open.
2. Plot the `calibrated_longwave_flux` variable.
    a. In the Panoply window with the list of NetCDF data fields, double click on **calibrated_longwave_flux**.
    b. The **Create Plot** dialog box will appear. The **Create a georeferenced Longitude-Latitude plot** radio button should already be checked by default.
    c. Click **Create**.
3. Format the plot area.
    a. Select the **Map** tab in the plot window.
        i. From the **Projection** drop down select **Stereographic**.
        ii. If you are plotting Northern Hemisphere data, set **Center on: Lon.** to -90 and **Center Lat.** to 90. If you are plotting Southern Hemisphere data, set **Center on: Lon.** to 0 and **Center Lat.** to -90.
    b. Select the **Scale** tab in the plot window.
        i. In the **Color Table** drop down, select **grayscale.act**.

Version History

Table 9. Version History

Version	Description
Version 1.0	Initial release of this data set.

Related Data Sets

Nimbus data sets from the Nimbus Data Rescue Project: The NIMBUS data rescue project, for early NASA satellite data, resulted in a number of related data sets and was the inspiration for this POES ESSA and NOAA series project. Meier et al. (2013) describe using it for estimates of sea ice extent in 1964.

Contacts and Acknowledgments

G. Garret Campbell was responsible for the development of this data product. He was assisted in scanning and navigating the imagery by University of Colorado students. The documentation and metadata were written by and are maintained by the NOAA@NSIDC program team. Ann Windnagel, as Product Owner, wrote most of the documentation, quality-checked files, and oversaw final assembly of the product at NSIDC.

The data are archived at NOAA NCEI and are made accessible through the OneStop system. Valerie Toner, NOAA Affiliate with the NCEI Archive Branch, was instrumental in helping us meet program requirements for archiving NetCDF data

with NCEI and other aspects of submitting data to the NCEI archive OneStop system. Jim Biard, NOAA Affiliate, worked with G. Garett Campbell extensively on issues related to NetCDF format compliance.

NOAA NCEI supported the development of this data product as part of NOAA participation in the inter-agency Big Earth Data Initiative (BEDI). BEDI funds were allocated to NOAA organizations to improve data discovery, accessibility, and usability, and to foster collaborations with NCEI that would ensure continuing preservation of the data. The project that produced this final data set began under the leadership of NOAA Data Management Architect Jeff de La Beaujardiere. This BEDI support was preceded by support in 2016 from the NCEI NOAA OneStop program under the leadership of Kenneth S. Casey, NCEI Deputy Director, Data Stewardship Division. NCEI's Dave Fischman was the Federal Principal Investigator partner on BEDI support and assisted throughout. NSIDC acknowledges the important role the administration of the NOAA BEDI and OneStop programs has played in shaping the final data product.

References

Kacker, R. and H. Yoon. 2015. Guidelines for Radiometric Calibration of Electro-optical Instruments for Remote Sensing. *NISTHB* 157. doi: http://dx.doi.org/10.6028/NIST.HB.157

Kalnay, E. et al. 1996. The NCEP/NCAR 40-year reanalysis project. *Bull. Amer. Meteor. Soc.* 77(3): 437-470.

Liebmann, B. and C. A. Smith. 1996. Description of a Complete (Interpolated) Outgoing Longwave Radiation Dataset. *Bull. Amer. Meteor. Soc.* 77(6): 1275-1277.
Note: The Interpolated OLR data from Liebmann and Smith (1996) was provided by the NOAA/OAR/ESRL PSD, Boulder, Colorado, USA, from their website at https://www.esrl.noaa.gov/psd/ in August 2018.

Massom, R. A. 1991. *Satellite Remote Sensing of Polar Regions: Applications, Limitations and Date Availability*. London: Bellhaven Press.

Meier, W. N., Gallaher, D., and G. G. Campbell. 2013. New estimates of Arctic and Antarctic sea ice extent during September 1964 from recovered Nimbus I satellite imagery. *The Cryosphere* 7: 699–705. doi: 10.5194/tc-7-699-2013. (Also see: NSIDC Highlights. 2013. *Glimpses of sea ice past*. https://nsidc.org/monthlyhighlights/2013/04/glimpses-of-sea-ice-past/.)

National Environmental Satellite Service. 1970. *Key to Meteorological Records Documentation No. 5.326: Catalog of Meterological Satellite Data – ESSA 9 and ITOS 1 Television Cloud Photography, April 1- June 30 1970*. Washington, D.C.: U.S. Dept. of Commerce - Environmental Data Service. (one of a series)

National Environmental Satellite Service. 1973. *Key to Meteorological Records Documentation No. 5.4: Environmental Satellite Imagery, January 1973*. Washington, D.C.: U.S. Dept. of Commerce - Environmental Data Service. (one of a series)

Additional References

The following references are taken from *Satellite Remote Sensing of Polar Regions: Applications, Limitations and Date Availability* by Robert Massom, published in 1991. They are included here in the hope that they will be useful to those doing research with the rescued ESSA and NOAA satellite data.

References listed in Massom (1991) Part 2, Details of Individual Satellites, ESSA 1-9

Booth, A. and Taylor, V. 1969. Meso-scale archive and computer products of digitized video data from ESSA satellites. *Bulletin of the American Meteorological Society* 50: 431-8.

Streten, N. 1968. Some aspects of high latitude southern hemisphere circulation as viewed by ESSA-3. *Journal of Applied Meteorology* 7(3): 324.

Streten, N. 1973. Satellite observations of the summer decay of the Antarctic sea ice. *Archiv für Meteorologie, Geophysik und Bioklimatologie Series* A, 22, 1: 119-34.

Swithinbank, C. 1971. Composite satellite pictures of the polar regions. *Polar Record* 15, 98: 743-4.

Taylor, V. and Winston, J. 1968. Monthly and seasonal mean global charts of brightness from ESSA 3 and ESSA 5 digitized pictures, February 1967 – February 1968. *ESSA Technical Report NESC 46,* Washington DC.

Wendler, G. 1973. Sea ice observation by means of satellite. *Journal of Geophysical Research* 78, 9: 1427-48.

References listed in Massom (1991) Part 2, Details of Individual Satellites, ITOS-1 and NOAA 1-5

Aber, R. and Vowinckel, E. 1972. Evaluation of North Water spring sea ice cover from satellite photographs. *Arctic* 25: 263-71

Ahlnas, K. 1979. IR enhancement techniques to delineate surface temperature and sea ice distributions. *Proceedings of the 13th International Symposium on Remote Sensing of the Environment,* 23-27 April 1979, Volume 1: 1,067-76. ERIM, Ann Arbor, Michigan.

Conlan, E. 1972. Operational products from the ITOS Scanning Radiometer data. *NOAA Technical Memorandum NESS 52.* US Department of Commerce, Washington DC.

DeRycke, R. 1973. Sea ice motions off Antarctica in the vicinity of the eastern Ross Sea as observed by satellite. *Journal of Geophysical Research* 73, 36:8,873-9

Gruber, A. 1977. Determination of the Earth-atmosphere radiation budget from NOAA satellite data. *NOAA Technical Report NESS* 76. NOAA, Department of Commerce, Washington DC.

Legeckis, R. 1978. A survey of worldwide sea surface temperature fronts detected by environmental satellites. *Journal of Geophysical Research* 83, 9: 4,501-22.

McClain, E. 1974. Some new satellite measurements and their application to sea ice analysis in the Arctic and Antarctic. In *Advanced concepts and techniques in the study of snow and ice resources*: 457-66. US National Academy of Science, Washington DC.

McGinnis, D., Pritchard, J. and Wiesnet, D. 1975. Determination of snow depth and snow extent from NOAA-2 satellite very high resolution radiometer. *Water Resources Research* 11: 897.

Streten, N. 1974. Large-scale sea ice features in the western Arctic basin and the Bering Sea as viewed by the NOAA-2 satellite. *Journal of Arctic and Alpine Research* 6, 4: 333-45.

Wiesnet, D. 1980. A satellite mosaic of the Greenland ice sheet. *World glacier inventory, Proceedings of the Riederalp Workshop,* September 1978. *International Association of Hydrological Sciences Publication* 126: 343.

Document Information

Author

A. Windnagel prepared this document with correspondence from G. Campbell and F. Fetterer.

Publication Date

June 2019; documentation updated October 2019

Appendix - Quality Differences for 35 mm Film, Glossy, and Halftone

There are three sources of analog images: 35 mm film, glossy prints, and halftone prints. Generally, the film/glossy prints resulted in image files with better quality, and these were used over the halftone prints, if available. To illustrate this, small versions the VIS images are shown in Figure 9. The images made from film/glossy prints (top) and those from halftone prints (bottom) do not look very different. However, when larger versions of the images are shown (Figures 10, 12, and 14), differences in quality become apparent. Figures 11, 13, and 15 show sections of these hemispheric images at full resolution. All of the raw image files, both those from film/glossy prints, and those from halftone prints, were mapped to the same 10 km grid, yet the true resolution of the halftone prints is coarser than 25 km. The Acquisition section has information on how ground resolution of the sensors and the resolution achievable using analog data varies, and why a 10 km grid was chosen.

Figure 9. Examples of 35 mm film (top left), glossy print (top right), and halftone prints (bottom). Note: the brightness in these VIS images has been enhanced to show detail. For larger versions, see Figures 10, 12, and 14, respectively.

Figure 10. VIS 35 mm film from 01 June 1967 (brightness has been enhanced to show detail).

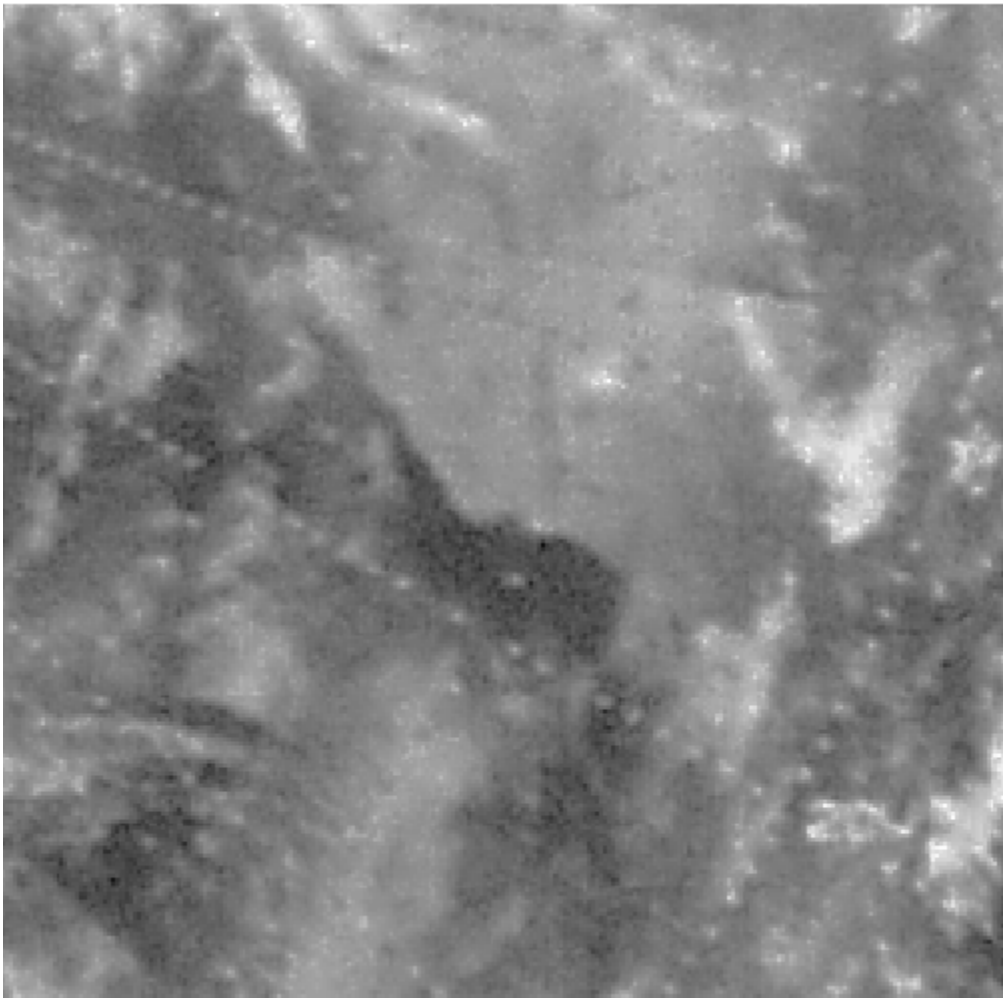

Figure 11. Section of the 35 mm film image shown in Figure 10 displayed at full screen resolution (brightness has been enhanced to show detail).

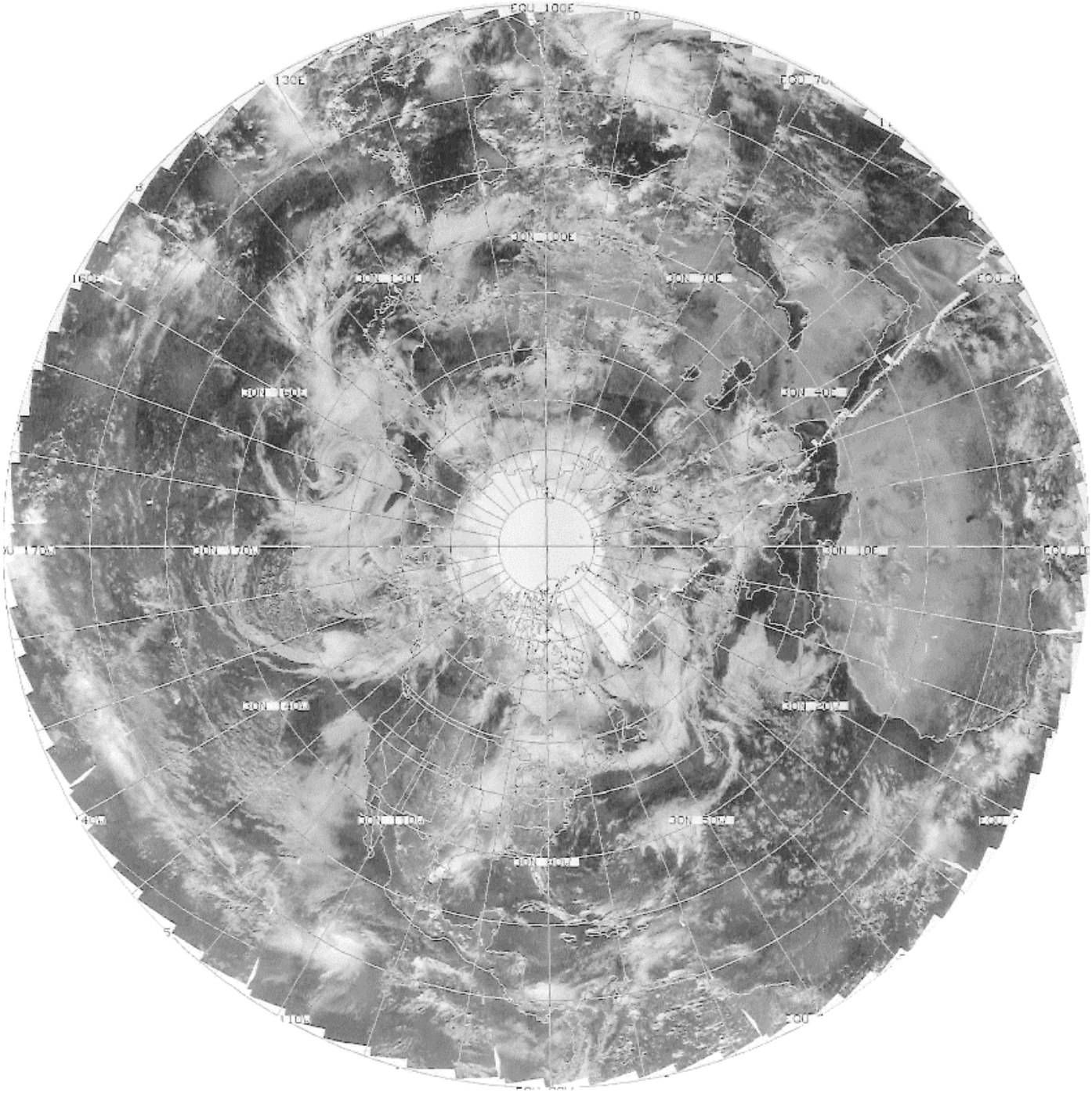

Figure 12. VIS glossy print from 01 June 1970 (brightness has been enhanced to show detail).

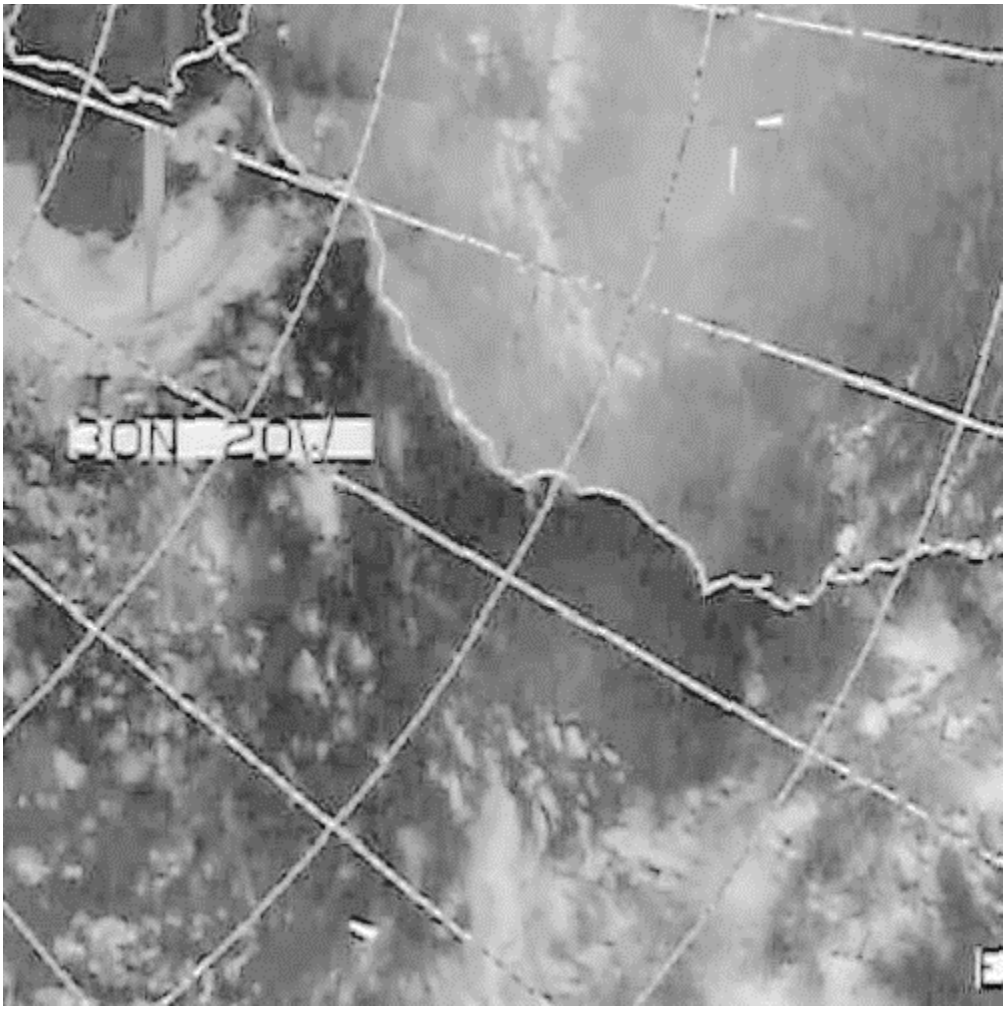

Figure 13. Section of the glossy print in Figure 12 displayed at full screen resolution (brightness has been enhanced to show detail).

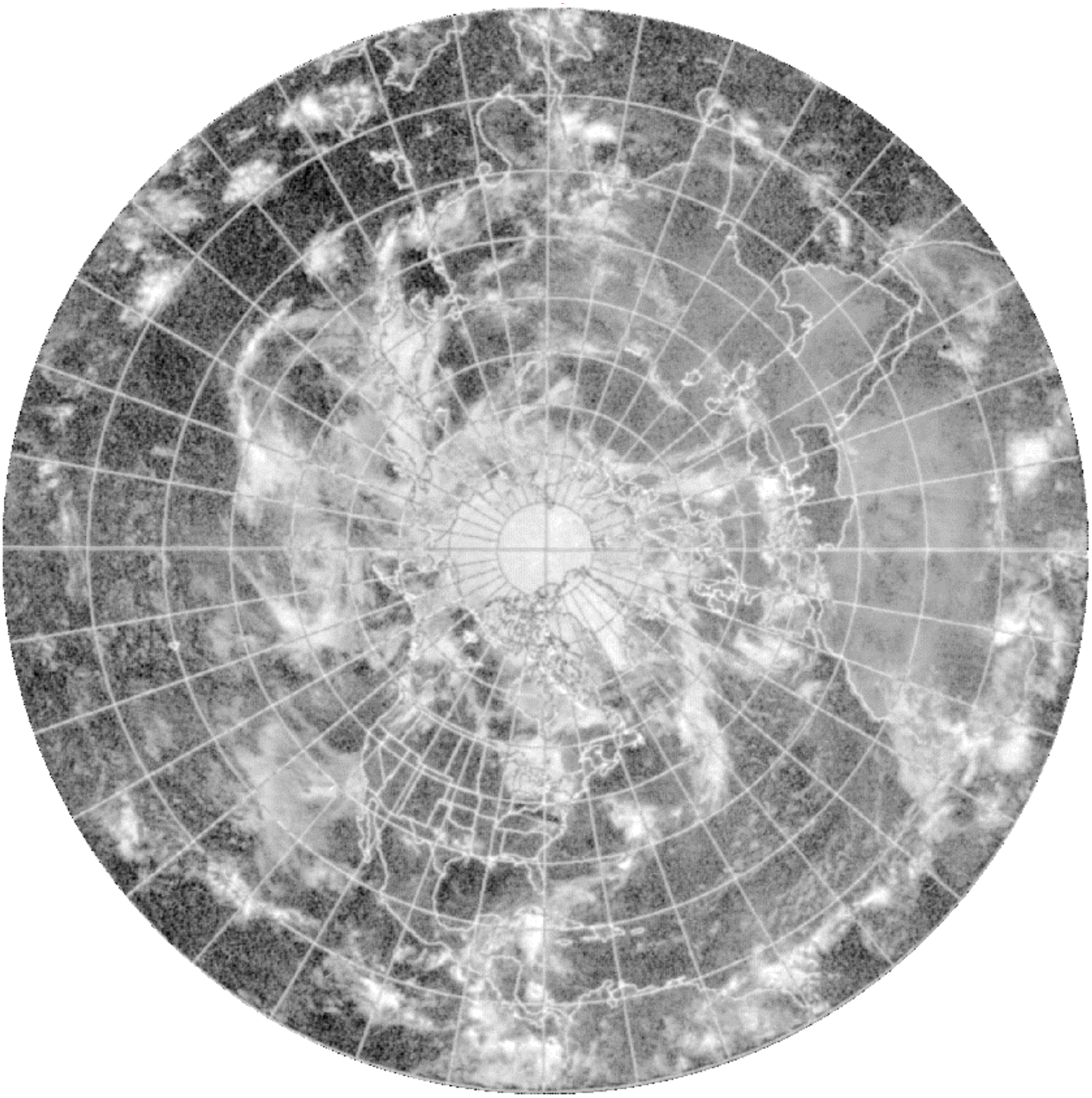

Figure 14. VIS halftone print from 01 June 1977 (brightness has been enhanced to show detail).

Figure 15. Section of the halftone print in Figure 14 displayed at full screen resolution (brightness has been enhanced to show detail).